Supplemental Information:

Quartz Crystal Microbalance as a tool for biomolecular interaction study

*Yuanzi Wu,[a] Hongwei Ma[a] , dayong Gu[b] and Jian'an He[b]**

[a] Suzhou Institute of Nano-Tech and Nano-Bionics, Chinese Academy of Sciences, Suzhou 215125, P. R. China. [b] Institute of Disease Control and Prevention, Shenzhen International Travel Health Care Center, Shenzhen Entry-exit Inspection and Quarantine Bureau, Shenzhen, 518033, P. R. China

*hejianan6398@163.com

*To whom correspondence should be addressed.

Table S1. A comparison between the values of fitted B and the values of ΔD for multi-step binding detections.

[SA] [a]	Low Density						High Density					
	SA		B-anti-IgG		IgG		SA		B-anti-IgG		IgG	
	B [b]	ΔD [c]	B [b]	ΔD [c]	B [b]	ΔD [b]	B [b]	ΔD [c]	B [b]	ΔD [c]	B [b]	ΔD [c]
100	0.1	-0.8	-0.3	1.5	-0.1	0.2	0.8	-2.0	-0.4	2.7	-0.3	1.3
50	0.1	-0.7	-0.3	1.4	-0.1	0.3	0.9	-2.2	-0.5	2.4	-0.2	1.0
20	0.1	-0.6	-0.2	0.9	-0.1	0.3	0.6	-2.4	-0.5	2.5	-0.2	1.0
10	0	-0.1	-0.1	0	-0.1	0	-0.3	0.6	0	0.2	-0.1	0.4

[a] unit is μg mL^{-1}, [b] unit is Hz, [c] unit is 10^{-6}.

Non-linear relation between A and [SA]:

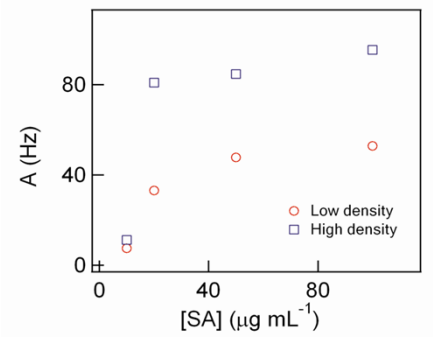

Figure S1. The A values were plotted again [SA], resulting a non-linear relation. It was attributed to the different binding mode (one SA to one biotin, or one to two, three, even four).

Table S2. List of fitted values of A and B, and calculated area averaged mass increase upon the addition of IgG at 20 μg mL^{-1} to different the B-anti-IgG captured biotin matrix.

[SA] [a]	Low Density					High Density				
	A [b]	**B** [b]	**Δm_1** [c]	**Δf** [d]	**Δm_2** [e]	**A** [b]	**B** [b]	**Δm_1** [c]	**Δf** [d]	**Δm_2** [e]
100	8.5	-0.1	153	7.9	142	14.0	-0.3	252	11.9	214
50	7.1	-0.1	128	6.5	117	12.3	-0.2	221	10.5	189
20	3.4	-0.1	61	3.0	54	9.1	-0.2	164	7.3	131
10	1.6	-0.1	29	0.2	3.6	1.6	-0.1	29	1.0	18

[a] unit is μg mL^{-1}, [b] unit is Hz, [c] the area averaged mass calculated according to equation 4. The unit is ng cm^{-2}, [d] average of 7 overtone numbers, $\Delta f = \Delta f_n/n$, n = 3, 5, 7, 9, 11 and 13. The unit is Hz, [e] the area averaged mass calculated according to equation 5. The unit is ng cm^{-2}.

Test of nonfouling property of the PEG matrices:

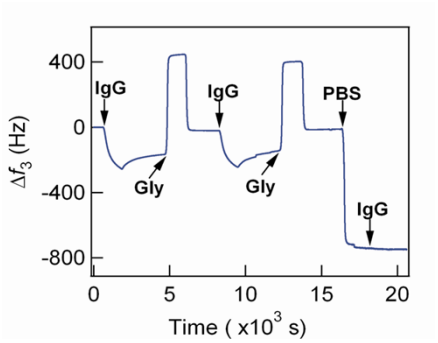

Figure S2. Nonfouling property of the PEG matrix. The PEG matrix coated QCM chip was first probed with HAc (2 mM, pH = 4.6) as the running buffer. Then, IgG (50 μg mL^{-1}) and Gly (100 mM, pH = 2.0) were introduced as indicated in figure, the frequency decrease (168.8 Hz) was due to the electrostatic adsorption (IgG (pI=8.0) has a positive charge when pH=4.6, while the PEG matrix has a negative charge.) After two cycles, PBS (pH = 7.4) was applied as the running buffer. No nonspecific adsorption ($\Delta f = 0$) was found upon the introduction of IgG (50 μg mL^{-1}). The experimental results indicated that, the nonspecific adsorption on QCM chips mostly resulted from the electrostatic adsorption. Meanwhile, the electrostatic adsorption plays a very important role in immobilizing proteins (especially when it is in a relatively low concentration), which enhances the enrichment of proteins on chip surfaces and promotes its immobilization ability. Therefore, we can regulate the ability of static interaction through control the amount of carboxyl group and buffer solution.

Optimization of experimental conditions for immobilization, binding and regeneration of the sensor chips (QCM and SPR):

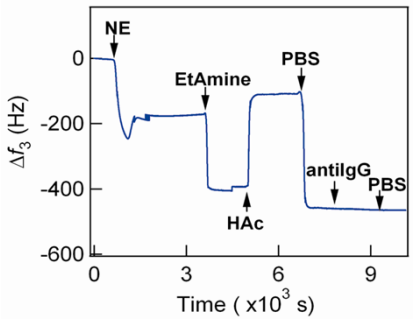

Figure S3. Efficiency of deactivation. For a COOH

functionalized QCM chip, it was first probed with HAc (2mM, pH = 4.6) as the running buffer, followed by NHSS/EDC (NE) activation. Ethanolamine (EtAmine, 1M, pH = 8.5) was directly applied to deactivate actived carboxyl groups. The running buffer was then switched to PBS (pH = 7.4), followed by flowing through anti-IgG (50 μg mL^{-1}), nonspecific adsorption was below the detection limit of QCM.

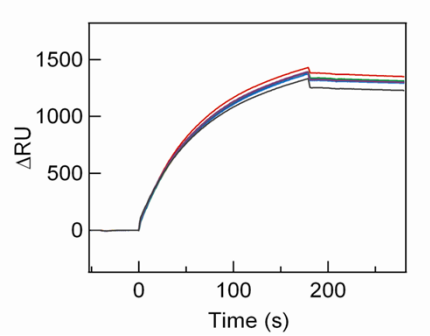

Figure S4. Regeneration study of COOH functionalized SPR sensor chips, the binding curves were reconstructed for clarity. The regeneration was reproducible and good for affinity and kinetic studies (Table S3).

Table S3. Regeneration study of SPR sensor chips.

	Anti-IgG (25μg mL^{-1})						
	0	1	2	3	4	5	6
ΔRU	1369	1317	1328	1307	1317	1314	1243
regeneration	100%	96.2%	97.0%	95.5%	96.2%	96.0%	90.8%

* IgG at 50 μg mL^{-1} was immobilized to sensor surface, resulting in ΔRU = 3588. The concentration was chosen so it matched with QCM experiments.

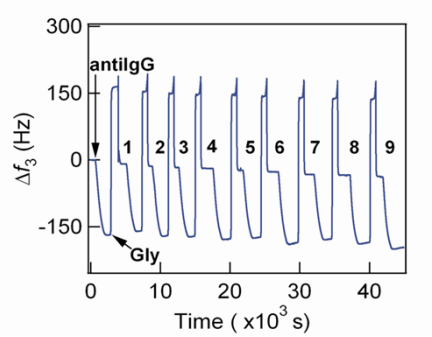

Figure S5. Regeneration study of COOH functionalized QCM sensor chips. The regeneration was reproducible and good for affinity and kinetic studies (Table S4).

Table S4. Regeneration study of COOH functionalized QCM chips (see Figure 4 in text and Figure S5 for detailed conditions).

NO.	0	1	2	3	4	5	6	7	8	9
Δf_3(Hz)	168.7	151.3	157.5	156.1	159.3	151.9	161.8	146.6	154.3	161.6
regeneration	100%	89.7%	93.3%	92.5%	94.4%	90.0%	95.9%	86.9%	91.5%	95.8%

Simulation of affinity and kinetic rate constants:

Analysis of binding experiments is based on a simple one to one binding model:

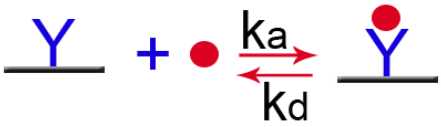

Scheme S1. A one to one binding model was applied to fit the QCM curve.

The reaction between immobilized bait (L) and a prey (P) can be assumed to follow a pseudo first order kinetics.

$$L + P \longleftrightarrow [LP] \qquad \text{(S1)}$$

The complex [LP] increases as a function of time according to:

$$\frac{d[LP]}{dt} = k_a \times [L] \times [P] - k_d \times [LP] \qquad \text{(S2)}$$

where k_a is the association rate constant and k_d is the dissociation rate constant

After a some time reaction

$$[L] = [L]_0 - [LP] \qquad \text{(S3)}$$

Substituting into Eq (S2), thus transformed as:

$$\frac{d[LP]}{dt} = k_a \times [P] \times ([L]_0 - [LP]) - k_d \times [LP] \qquad \text{(S4)}$$

It was assumed that frequency change has a linear relation with captured prey molecules. So rewriting the formula in the term of frequency responses and concentration:

$$\frac{df}{dt} = k_a \times C \times (f_{\max} - f) - k_d \times f \qquad \text{(S5)}$$

Where C is the concentration of the free prey, f is the frequency responses. $f_{\max}$ is the max frequency responses.

After integration, we can get:

$$\Delta f = \frac{k_a C \Delta f_{\max}}{(k_a C + k_d)} (1 - e^{-(k_a C + k_d) \times t}) \qquad \text{(S6)}$$

Let:

$$Y = \frac{k_a C \Delta f_{\max}}{(k_a C + k_d)} \; ; \quad Z = k_a \times C + k_d \qquad \text{(S7)}$$

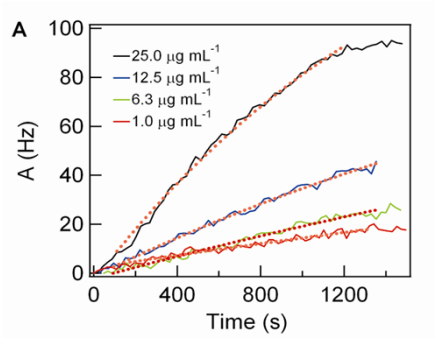

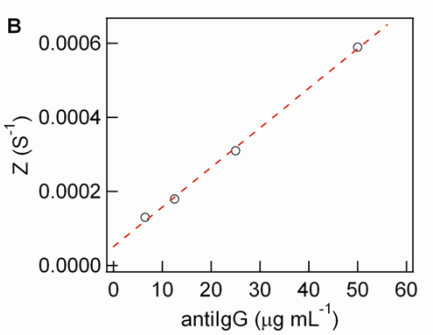

Figure S6. The curve of fitted A fitting for affinity and kinetic constants determination. (A) kinetic simulation based on fitted A values; (B) the fitted values of Z were linearly fitted, resulting in k_a=5.0×10^{-5}μg^{-1} mL s^{-1}, k_d=1.1×10^{-5} s^{-1}and $K_A = k_a/k_d$=6.8×10^8 M^{-1}, R^2=0.998

Table S5. The affinity and kinetic rate constants were independent on overtone number, n.

n	3	5	7	9	11	13
k_a (μg^{-1} mL s^{-1})	4.0×10^{-5}	5.0×10^{-5}	5.0×10^{-5}	4.0×10^{-5}	5.0×10^{-5}	4.0×10^{-5}
k_d (s^{-1})	5.0×10^{-5}	3.0×10^{-5}	4.0×10^{-5}	3.0×10^{-5}	5.0×10^{-5}	2.0×10^{-5}
K_A (M^{-1})	1.2×10^{8}	2.8×10^{8}	1.9×10^{8}	2.0×10^{8}	1.5×10^{8}	3.0×10^{8}
R^2	0.999	0.999	0.995	0.999	0.997	0.999

*The procedure for bait immobilization (IgG at 25 μg mL^{-1}) was the same as Figure 4. Anti-IgG at a series of concentrations ((1) 1.0 μg mL^{-1}; (2) 6.3 μg mL^{-1}; (3) 12.5 μg mL^{-1}; (4) 25.0 μg mL^{-1}; (5) 50.0 μg mL^{-1}) and Gly (100 mM, pH = 2.0) were introduced in turns.

Affinity and kinetic rate constants determined by SPR:

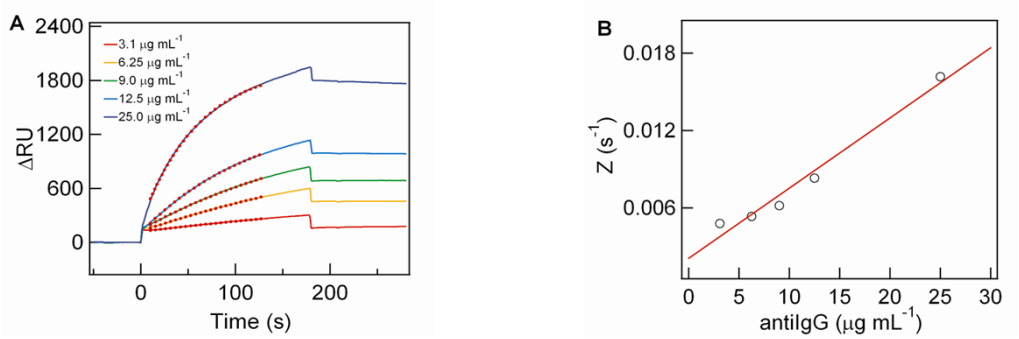

Figure S7. Curve fitting for affinity and kinetic constants determination by SPR. IgG at 50 μg mL^{-1} was immobilized to sensor surface, resulting in ΔRU = 3588. The concentration was chosen so it matched with QCM experiments. (A) the binding curves were reconstructed for clarity and fitted according equations (11) and (12); (B) the fitted values of Z were linearly fitted, resulting in k_a, k_d and K_A, see Table S6 for numbers.

Table S6. Affnity and kinetic rate constants for the binding between IgG and antiIgG

Bait	prey	k_a(μg^{-1} mL s^{-1})	k_d (s^{-1})	K_A (M^{-1})	R^2
IgG	Anti-IgG	5.0×10^{-4}	2.1×10^{-3}	3.6×10^{7}	0.974

Anti-IgG	IgG	1.3×10^{-3}	6.6×10^{-3}	3.0×10^{7}	0.964

*IgG at 50 μg mL^{-1} was immobilized to sensor surface, resulting in ΔRU = 3588. The concentration was chosen so it matched with QCM experiments.

The choice of bait was critical:

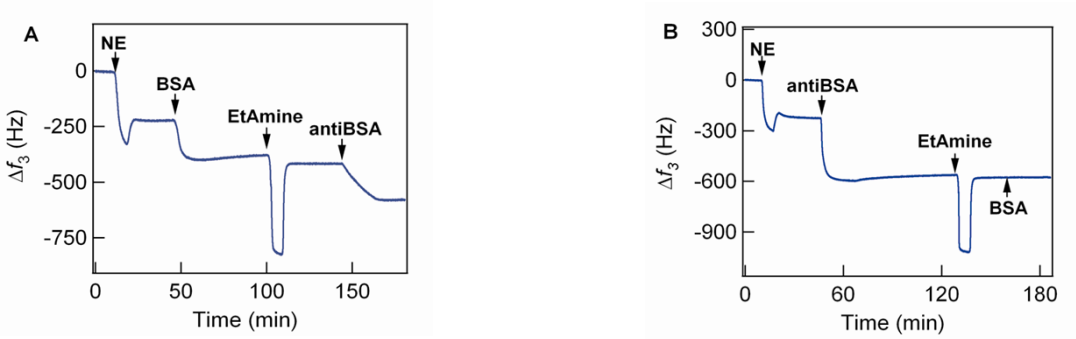

Figure S8. Bait-prey recognition curves for BSA and anti-BSA pairs. The standard procedure was described in detail in Figure 1 of text. (A) BSA (100 μg mL^{-1}) was immobilized on a COOH functionalized QCM chip and anti-BSA (1 μg mL^{-1}) was passed through. There was a 161.8 Hz frequency decrease due to bait-prey recognition, (B) The immobilization of anti-BSA as the bait at 10 μg mL^{-1} resulted in 340 Hz frequency decrease. No frequency decrease was found when anti-BSA (10 μg mL^{-1}) was passed through as prey.

2D matrix vs. 3D matrix:

We did the same study on $(EG)_3$-SAM as matrix, the results of which indicated: (i) the regeneration of $(EG)_3$-SAM matrix was better than that of COOH functionalized PEG matrix. For an $(EG)_3$-SAM matrix with only one single layer of COOH, the protein immobilized to it could be easily removed (Table S7); (ii) three dimensional matrix could enhance the ability of immobilization of bait molecules, with a better nonfouling property as well (Figure S9).

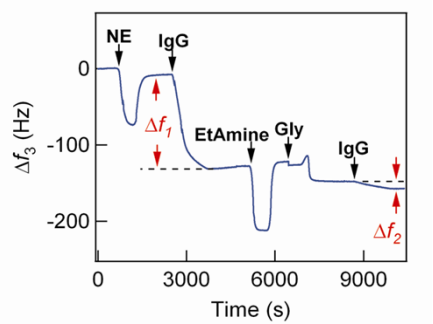

Figure S9. The detection of the immobilized ability and the nonspecific ability for **(**$(EG)_3$-SAM. For an $(EG)_3$-SAM QCM chip, it was first probed with HAc (2 mM, pH = 4.6) as the running buffer, followed by NHSS/EDC (NE) activation. Then, IgG (50 μg mL^{-1}) was introduced, resulting in a 122.6 Hz frequency decrease. Ethanol amine (EtAmine at 1 M, pH = 8.5) was applied to deactivate remaining active carboxyl groups. The running buffer was then switched to Gly (100 mM, pH = 2.0), followed by flowing through IgG (50 μg mL^{-1}) in order to test the nonfouling property of the $(EG)_3$-SAM, resulting in a 9.5 Hz frequency decrease.

Table S7. Regeneration study of $(EG)_3$-SAM QCM chips

No.	0	1	2	3	4	5
Δf_3 (Hz)	161.9	158.2	154.0	151.8	157.7	158.0
regeneration	100%	97.7%	95.1%	93.8%	97.4%	97.6%

Reference:

(1) Fu, L.; Chen, X. A.; He, J. A.; Xiong, C. Y.; Ma, H. W. *Langmuir* **2008**, *24*, 6100-6106.